Study of Radon Propagation in A Dwelling Using the CFD Modelling Capabilities of CONTAM

Javier García-Tobar

Polytechnic University of Madrid, School of Mining and Energy Engineering

jgtobar@iies.es

Abstract

Naturally occurring radon gas is the leading cause of lung cancer for nonsmokers. Limiting the amount of radon inhaled by residents when designing homes and HVAC systems is of utmost importance. This report focuses on dedicated 3D CFD simulations of indoor radon distribution in a dwelling located in Madrid, Spain, using the CONTAM and CFD-0 software developed by NIST. CFD can be used and has many advantages for indoor air flow analysis with reduced mathematical limitations. The results are qualitative and show the possibility to calculate detailed volumetric radon concentrations inside a ventilated dwelling. This technique allows a better estimate of the radon infiltration rate to mitigate the accumulation of radon inside dwellings.

Keywords: Radon, Computational Fluid Dynamics, Modelling, Indoor Air Quality

Introduction

Radon (^{222}Rn) is a chemically inert radioactive gas with a 3.8 day half-life produced naturally in the decay chain of ^{238}U. It can be found everywhere on the Earth's surface in different concentrations, being accumulated mostly in poorly ventilated environments [1]. Radon emission is massively influenced by the geological structure and characteristics that are seen in bedrock [2]. Inhalation of radon and their decay products constitute the largest fraction (52%) of radiation dose received by humans from natural background radiation [3]. Measurement of indoor radon concentration is important due to the impact that radon can have on indoor air quality and the health effects that this can have through inhaling that air.

A fundamental tool to design effective radiation protection strategies against radon is mapping the most exposed geographical areas. The mapping of the radon potential in Spain, developed by the Nuclear Safety Council, categorizes the areas according to their indoor radon levels and identifies those in which a significant percentage of residential buildings that have concentration levels higher than 300 Bq / m^3 [4]. The presence of indoor radon varies depending on the uranium content of the soil and, in Spain; it is more frequent in Galicia, certain areas of Castilla and León, Northern Extremadura and Northern Madrid. Within the Community of Madrid, the highest levels of exposure are identified with the granite outcrops on the southern slopes of the Gredos mountain range, and with the granite alterite mantles of the Sierra de Guadarrama [5].

The Council Directive of 2013/59/EURATOM has promoted in Spain, the development of a new basic document, the Technical Building Code which relates to protection against radon [6]. This new document classifies municipalities as having high, moderate or low potential for indoor radon problems. Community of Madrid has over 100 municipalities, such as, El Escorial, Brunete, Cercedilla, Guadarrama, Moralzarzal, Rascafría and Torrelodones.

A comparative study of indoor radon level in two similar dwellings in Madrid was also conducted based on simulation performed with the multi-zone modelling software CONTAM developed by the National Institute of Standards and Technology (NIST) [7, 8]. The survey found that the average radon concentration is over 60-80 Bq/m^3. This work presents a technique for estimating radon levels in the different rooms of two dwellings using the CONTAM modelling software and investigates the generation rate of indoor radon sources relative to the total surface of each room [7]. A comparison of the simulated indoor radon levels helped identifying the rooms that required special attention. Simulations for different fan airflow levels were also performed for a specific room and the impact in the radon concentrations was analyzed. The CONTAM software and methodology

presented should be a help in accomplishing the requirements from Council Directive 2013/59/EURATOM [9], as part of arranging for the establishment of strategies to ensure the appropriate management of existing exposure situations commensurate with the risks and with the effectiveness of protective measures required in Articles 101 and 103.

There's a good agreement between simulated and measured values of radon concentrations for the two dwellings when including weather factors such as outdoor temperature, barometric pressure, wind speed and wind direction [10]. The main variations of indoor radon levels were shown to originate mainly from meteorological factors. A correlation was established between low/high barometric pressure, outdoor temperature or indoor–outdoor temperature difference and low/high radon concentrations, with these observations reflected in both simulated and measured datasets [10].

In the recent years, Computational Fluid Dynamics (CFD) has shown great promise for simulation of indoor radon problems [11]. Compared to multizone models, CFD methods use fewer assumptions and are able to obtain detailed spatial values of airflow and contaminant concentrations. CFD solves the governing fluid equations and provides spatial and temporal field solution of variables such as pressure, temperature and energy density. It also provides velocity flow fields and the dispersion pattern of indoor pollutant [11]. One of the drawbacks of CFD is that it demands a lot more computing time than the multizone models [12]. To achieve fast computing speed, a number of assumptions must be made regarding zone parameters and airflow characteristics. The idea of multizone-CFD coupling is to apply a multizone program to most zones of a building while applying a CFD program to the zones where the multizone assumptions are not appropriate.

In the simplified approach observed in this work, most components are modeled using the CONTAM multizone network program, and provided detailed CFD analysis only to a specific zone, where the simplified "well-mixed" assumption may not stand. This approach was possible thanks to Wang and Chen [12, 13] who coupled CONTAM with CFD-0, a CFD code, originally developed by Srebric et al. [14].

Multizone airflow network models and CFD have been widely used in simulations of building airflow distribution and contaminant transport. A number of recent papers show a promising descriptive and predictive power of CFD simulations for radon in various environments through comparisons with measurement [11, 13]. Using CFD modelling, the spatial distribution of radon in test room conditions was simulated and found that radon distribution was unequal due to the difference in the flux from different sources in non-mixing conditions [11]. This can also been seen through the example case of coupling CFD and multi-zone models in which it was assessed through the effects of driving speed and tailpipe location on pollutant levels inside a school bus as a result of self-pollution [14]. This model has shown reasonable results for the school bus cabin, although there were some disagreements in the predictions for the front of the cabin. CFD-0 module of the CONTAM software simulated the airborne contaminant transport in the healthcare industry and throughout hospitals and laboratory applications [15]. One of the most comprehensive studies showed and took into consideration different indoor variables such as temperature, ventilation rate and humidity for the 3D CFD simulations [18]. It was shown that the indoor radon level was reduced with the ventilation rate, as well as, when the gradient of temperature between inside and outside increases. On the other hand, it increased with increasing relative indoor humidity.

The aim of this paper is to develop a methodology for determining the impact of weather effects to the distribution of radon concentration within a room based on 3D CFD simulations. The Tecplot software [16] will be used to display results in a user-friendly manner such that radon mitigation decisions can be taken based on the graphical outputs.

Methodology

Multizone network models employ several assumptions, which may lead to inaccurate results in flow calculations, such as: uniform pressure at the same height of a zone, uniform temperature, uniform contaminant

concentration in a zone, airflow through zones does not impact zone pressure, momentum and kinetic energy not accounted for by flow path models, and well-mixed air composition when determining contaminant concentrations. These assumptions can be eliminated in the zones where they are inappropriate by coupling a multizone network program with a CFD program.

CFD allows one to calculate detailed non-uniform spatial distributions for air momentum contaminant concentration and/or air temperature by solving the governing conservation equations. A simulation of a whole building at steady-state conditions can take several hours or even days, therefore, CFD is not feasible for hour-by-hour dynamic simulations for long periods of time. One could use CFD for those zones where the uniform assumptions would fail so the accuracy of the simulated results can be greatly improved, compared with using a multizone model alone. The use of a multizone method applied with a CFD method can combine their advantages and avoid and outweigh their drawbacks. On the other hand, CFD is only applied to smaller areas meaning that the computing time with the coupled program would be more manageable, compared with using a CFD model alone for the whole building.

Wang and Chen [12] established two necessary conditions for a successfully coupled airflow calculation with CONTAM and CFD:

(1) Mass airflow rate predicted by a multizone airflow network model must equal the integral of the mass airflow rate of all CFD grid cells for each interface airflow path to ensure overall mass balance.
(2) The resistance characteristic (i.e., the airflow rate as a function of pressure drop) must be known for each multizone/CFD boundary grid cell to ensure closure of the problem.

In the CFD program, a set of partial differential governing equations for mass, momentum, and energy conservation are solved, as noted in Ref. [12], leading to the total matrix equation:

CP + F = B

where **C** represents the CFD coefficient matrix, **P** is the unknown pressure vector of zones and cells, **F** is the vector of unknown flow rates at interface paths and cells and **B** represents the vector of air mass sources. The solving procedure is realized iteratively between CONTAM – CFD-0 – CONTAM so that the output of one program becomes the input of the other. When both inputs do not change between two iterations, the solution of the coupling is considered convergent and the calculation proceeds to the next time step.

The living room is so large that the homogeneous assumption is inappropriate and is therefore chosen as the CFD zone while the remaining zones are modelled with the multizone program [7, 10]. This apartment was located on the 1st floor of a residential building in the neighborhood of a district in Madrid (the Salamanca district) Guindalera and can be found with the location and coordinates of latitude 40° 26' 24" N and longitude 3° 40' 12" W.

Figure 1 shows, side-by-side, the CONTAM multizone sketch for the entire dwelling comprising of 4 zones, and the CFD-0 sketch for the living-room defined as a CFD zone. The software used is CONTAM with CFD-0 version 3.2, developed by NIST [8, 17]. The CFD region corresponding to the living room also includes the kitchen, being an open-space type of living room, and the bathroom walls in order to be able to define all their corresponding interface elements. The parameters for the multizone simulation including weather effects are identical to the ones defined in Ref. [7]. The rectangular dimensions of the living room together with the bath and small corridor used as input for CFD-0 are as following: 9 m (L) x 3.2 m (W) x 3 m (H). A total number of 15,120 control volumes have been defined by dividing the entire volume of the CFD region into a grid of 42 (L) x 24 (W) x 15 (H) cells.

A radon sink was defined in the hallway in order to study the infiltration rate and path followed by radon in the living-room. The generation rate of the sink was set to 1.8×10^5 Bq/h in order to provide an average radon concentration in the living room of 70 Bq/m^3 in the absence of any weather effects [7]. When weather effects

are included, radon concentrations fluctuate between few tens and beyond 100 Bq/m^3 [10]. It should be noted that in reality, sources of radon are more complex and have not been implemented in this simulations, since the purpose was to perform a qualitative study of the impact of weather effect on radon infiltration in a dwelling from a particular outside source, such as a hallway that is poorly ventilated.

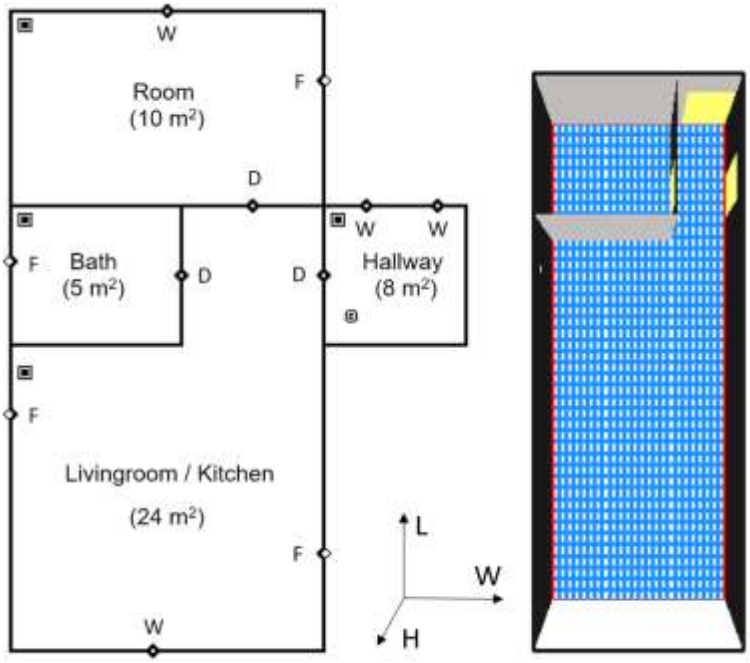

Fig. 1. (a) CONTAM and (b) CFD-0 drawings of the entire dwelling and bath together with the living room.

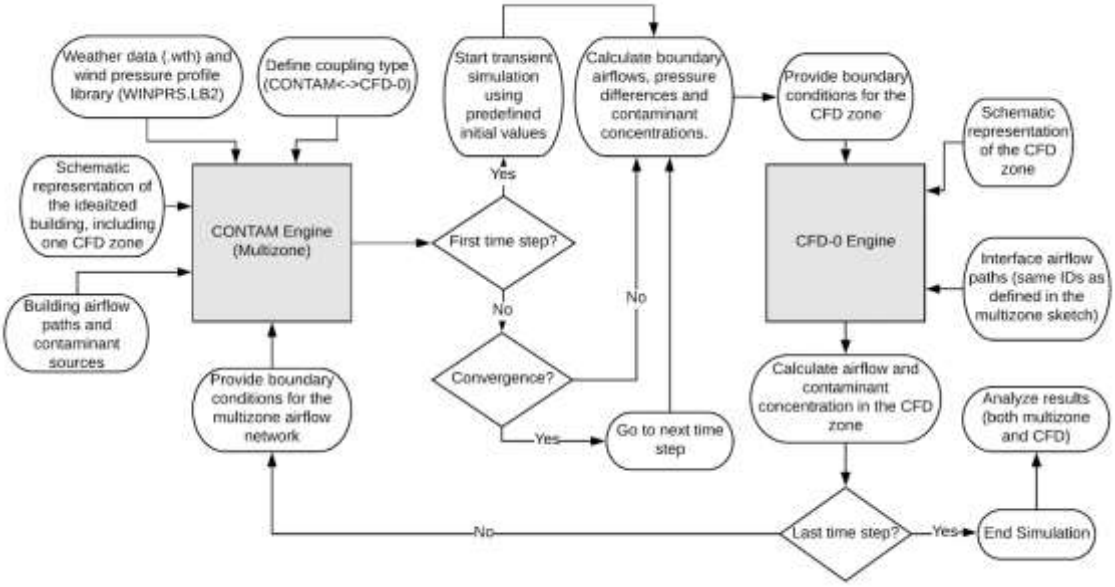

Fig. 2. Simplified flowchart showing the working principle of the coupling used in the present simulation between CONTAM and CFD-0.

The fully coupled procedure employed in the present paper, shown schematically in Fig. 2, obtains initial values of air pressures and flow rates for all zones by running a CONTAM simulation for the whole building. With boundary conditions from CONTAM, CFD-0 calculates the airflow in the CFD zone and feeds boundary

conditions back to CONTAM. The iteration continues until convergence is achieved for both sets of calculations. A convergence criterion of 0.01 was employed and the number of iterations was set to 100. Since radon was defined as a contaminant the same iterative procedure is used except that the contaminant concentration is exchanged at each interface airflow path. A detailed flowchart of the coupling when contaminant transport is required was provided in Fig. 2 [18]. For a coupled transient simulation, the procedure is repeated for each time step.

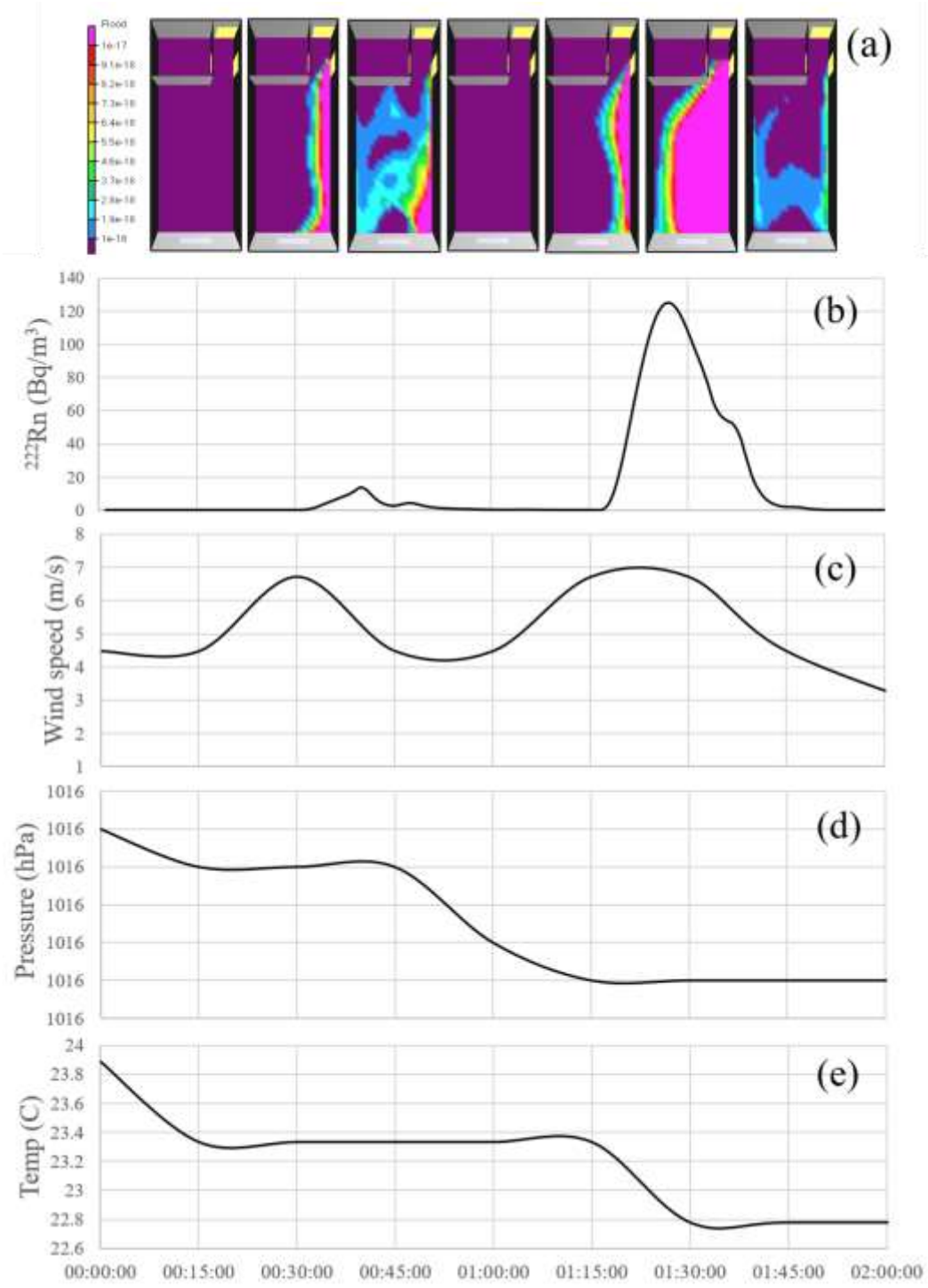

Fig. 3. Radon concentration in the living room simulated with (a) CFD-0 and (b) CONTAM for a 2h period. The outdoor conditions which have been shown to have a significant impact in the radon concentration are displayed, such as (c) wind speed, (d) pressure and (e) temperature.

In order to visualize the results of CFD calculations, the NIST CFD-0 program offers a limited interface based on 2D slices of the calculated volume (shown in Fig. 3). However, the results can be exported in a format compatible with commercial software that are much more capable in viewing and interpreting the results, including 3D high-resolution animated renderings. In the case of the present study, Tecplot 360 was used which is a CFD and numerical simulation software package used in post-processing simulation results [16], with numerous applications including aerodynamics, geoscience, internal combustion simulations, etc.

Results and Discussion

The present results include both CONTAM and CFD transient simulations for a 2h period during the day, including weather effects. Only the infiltration of radon from the hallway is treated in the current simulations, all the other sources such as outside radon, and exfiltration through building cracks or exhalation of radon from building materials have been neglected. In reality, all these effects are cumulative.

Figure 3 shows how radon infiltrates from the hallway into the living room towards the window. The main drive of external radon appears to be the instantaneous pressure difference caused by variable wind conditions, noted also in [19, 20].

The maximum radon concentration appears to overlap with the maximum wind speed, most probably due to a favorable wind direction which created a negative pressure area outside the window. The other factors have a much smaller influence, as it has been shown in the previous study [10]. The variation caused by temperature fluctuation have roughly a factor 10 weaker impact compared to the wind and external barometric pressure fluctuation an even lower impact than the variation induced by temperature.

In the case of CFD calculations, shown in Fig. 4, both steady and variable weather conditions have been simulated. In the steady weather simulation, the radon fills the room in roughly 2 hours reaching a relatively uniform concentration all across the room representing the equilibrium conditions. In the case of the variable weather simulation, the radon originating from the hallway enters the room abruptly with every pressure change due to the variable wind conditions but then it is quickly removed, in a matter of minutes, as indicated through the 15 minutes intervals from Fig. 3.

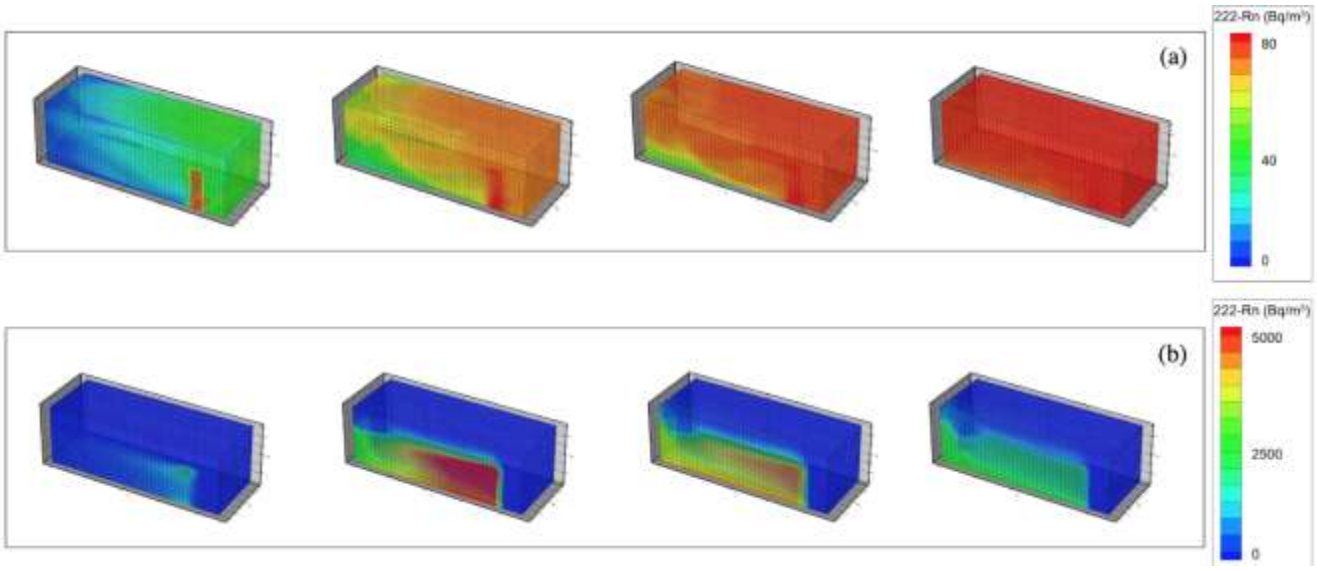

Fig. 4. Tecplot 360 [16] rendering of radon concentration in the living room simulated with CFD-0 considering (a) steady weather conditions and (b) variable weather conditions including wind. The same 2h period as in Fig. 3 was used.

Zones of increased radon concentration are present in the variable weather conditions, alongside the wall, indicating possible regions to avoid for prolonged human stationing and optimal places where radon monitoring sensors should be placed. These findings are similar to the ones reported in [11] where the spatial distribution of radon in the room was simulated using CFD and compared with measurements. It was observed that, radon distribution was not uniform due to the difference in the flux from different sources in non-mixing conditions.

Conclusions

This study has shown the opportunity of performing CFD calculations in order to determine volumetric concentrations of radon inside a dwelling. It has shown qualitatively that weather effects are of major importance in determining zones of higher radon concentrations inside a room. In the case of steady weather conditions, a uniform distribution is encountered, as expected and confirmed in previous studies.

Future studies are required in order to measure precisely radon concentration distributions inside rooms and validate CFD simulations of radon transport. Experimental validating of such simulations will allow a better estimate of the radon infiltration rate in order to mitigate the accumulation of radon inside dwellings and optimize the areas for human habitation.

References

1. N. Segovia and J. Cejudo, "Radon measurements in the interior of household dwellings," Nuclear Tracks and Radiation Measurements (1982), vol. 8, p. 407–410, 1984. https://doi.org/10.1016/0735-245x(84)90131-5
2. V. Sundal, H. Henriksen, O. Soldal and T. Strand, "The influence of geological factors on indoor radon concentrations in Norway," Science of the Total Environment, vol. 328, p. 41–53, 2004. https://doi.org/10.1016/j.scitotenv.2004.02.011
3. UNSCEAR, "Exposures of Workers and the Public from Various Sources of Radiation. Report A/AC.82/-644," in United Nations Scientific Committee on the Effects of Atomic Radiation, New York, 2000. https://doi.org/10.18356/46eef4a3-en
4. Spanish Nuclear Safety Council (CSN), "Mapa del potencial de radón en España," 2020. [Online]. Available: https://www.csn.es/en/mapa-del-potencial-de-radon-en-espana. [Accessed 19 March 2020].
5. L. S. Quindós, J. Soto, P. L. Fernandez, C. Rodenas, J. Gomez, J. Arteche, G. Romero and J. Madrid, "Radon and lung cancer in Spain," Radiation Protection Dosimetry, vol. 36, p. 331–333, 1991. https://doi.org/10.1016/0169-5002(92)90221-5
6. Boletín Oficial del Estado, Real Decreto 314/2006, de 17 de marzo, por el que se aprueba el Código Técnico de la Edificación, 2019. [Online]. Available: https://www.boe.es/buscar/act.php?id=BOE-A-2006-5515. [Accessed 19 March 2020].
7. J. García-Tobar, "A comparative study of indoor radon levels between two similar dwellings using CONTAM software," Environments, vol. 5, p. 59, 2018. https://doi.org/10.3390/environments5050059
8. W. S. Dols and B. J. Polidoro, "Contam user guide and program documentation version 3.2," 2015. https://doi.org/10.6028/nist.tn.1887
9. Directive, 59/Euratom of 5 December 2013 laying down basic safety standards for protection against the dangers arising from exposure to ionising radiation, and repealing Directives 89/618/Euratom, 90/641/Euratom, 96/29/Euratom, 97/43/Euratom and 2003/122/Euratom, Euratom, 2013.

10. J. García-Tobar, "Weather-dependent modelling of the indoor radon concentration in two dwellings using CONTAM," Indoor and Built Environment, vol. 28, p. 1341–1349, 2019. https://doi.org/10.1177/1420326x19841119
11. N. Chauhan, R. P. Chauhan, M. Joshi, T. K. Agarwal, P. Aggarwal and B. K. Sahoo, "Study of indoor radon distribution using measurements and CFD modeling," Journal of environmental radioactivity, vol. 136, p. 105–111, 2014. https://doi.org/10.1016/j.jenvrad.2014.05.020
12. L. Wang and Q. Chen, "Validation of a coupled multizone-CFD program for building airflow and contaminant transport simulations," HVAC&R Research, vol. 13, p. 267–281, 2007. https://doi.org/10.1080/10789669.2007.10390954
13. L. Wang and Q. Chen, "Theoretical and numerical studies of coupling multizone and CFD models for building air distribution simulations," Indoor Air, vol. 17, p. 348–361, 2007. https://doi.org/10.1111/j.1600-0668.2007.00481.x
14. J. Srebric, Q. Chen and L. R. Glicksman, "Validation of a zero-equation turbulence model for complex indoor airflow simulation," ASHRAE Transactions, vol. 105, p. 414, 1999.
15. N. Chauhan and R. P. Chauhan, "Active-passive measurements and CFD based modelling for indoor radon dispersion study," Journal of environmental radioactivity, vol. 144, p. 57–61, 2015. https://doi.org/10.1016/j.jenvrad.2015.03.009
16. F. Li, E. S. Lee, J. Liu and Y. Zhu, "Predicting self-pollution inside school buses using a CFD and multi-zone coupled model," Atmospheric Environment, vol. 107, p. 16–23, 2015. https://doi.org/10.1016/j.atmosenv.2015.02.024
17. B. P. P. Barbosa and N. d. C. L. Brum, "Validation and assessment of the CFD-0 module of CONTAM software for airborne contaminant transport simulation in laboratory and hospital applications," Building and Environment, vol. 142, p. 139–152, 2018. https://doi.org/10.1016/j.buildenv.2018.06.013
18. [18]R. Rabi and L. Oufni, "Study of radon dispersion in typical dwelling using CFD modeling combined with passive-active measurements," Radiation Physics and Chemistry, vol. 139, p. 40–48, 2017. https://doi.org/10.1016/j.radphyschem.2017.04.012
19. Tecplot 360, "Data Validation and CFD post-processing software," Tecplot USA, [Online]. Available: https://www.tecplot.com/. [Accessed 19 March 2020].
20. L. L. Wang, W. S. Dols and Q. Chen, "Using CFD capabilities of CONTAM 3.0 for simulating airflow and contaminant transport in and around buildings," Hvac&R Research, vol. 16, p. 749–763, 2010. https://doi.org/10.1080/10789669.2010.10390932
21. W. J. Riley, A. L. Robinson, A. J. Gadgil and W. W. Nazaroff, "Effects of variable wind speed and direction on radon transport from soil into buildings: model development and exploratory results," Atmospheric Environment, vol. 33, p. 2157–2168, 1999. https://doi.org/10.1016/s1352-2310(98)00374-4
22. G. Roserens, H. U. Johner, G. Piller, P. Imbaumgarten, A. Binz, F. Fregnan and G. Lehmann, "Swiss Radon Handbook," Swiss Federal Office of Public Health, Bern, 2000.